PAPER

Electronic structure calculations for rhenium carbonitride: an extended Hückel tight-binding study

IOP Publishing Physica Scripta
Phys. Scr. 93 (2018) 115801 (8pp) https://doi.org/10.1088/1402-4896/aae14c

Electronic structure calculations for rhenium carbonitride: an extended Hückel tight-binding study

Etienne I Palos, José I Paez, Armando Reyes-Serrato and Donald H Galván

Centro de Nanociencias y Nanotecnología, Universidad Nacional Autónoma de México, Apdo. Postal 14, 2280 Ensenada B.C., México

E-mail: g5_palo16@cnyn.unam.mx

Received 24 April 2018, revised 23 August 2018
Accepted for publication 13 September 2018
Published 5 October 2018

Abstract

Effective theoretical models are needed to predict the physical properties of materials. Here we discuss the electronic structure of rhenium carbonitride (ReCN) in terms of tight-binding. The extended Hückel tight-binding (EHTB) formalism was employed to calculate the band structure, density of states (DOS) and investigate the chemical bonding properties as well as the crystal field splitting (CFS) of *d* orbitals in the Re atom. Two ReCN structures were studied, characterized by space groups P63mc and P3m1, respectively. The calculated energy bands and DOS depict semiconductor properties for both structures, seeing an indirect band-gap of 0.62 eV in P63mc ($M - K$) while a direct band-gap of 0.49 eV is seen in P3m1 at (H). Mulliken population and CFS analysis were done to gain insight into the filling of 5*d* orbitals in ReCN, crystallographical differences between the two crystal structures and their physical implications. The five-fold degenerate energy levels in both the P63mc and P3m1 structures are broken by a tetragonal crystal electric field. The P63mc structure undergoes Peierls distortion, resulting in a loss of symmetry. The EHTB method is an effective tool to approximate the physical and chemical properties of novel materials such as ReCN at a low computational cost and in terms of a simple quantum-mechanical framework, understood by the broader community. The EHTB model for ReCN will serve as a benchmark and starting point for future studies on the compound within similar contexts.

Keywords: electronic structure, tight-binding, extended Hückel, ReCN, crystal field splitting, molecular orbital theory

(Some figures may appear in colour only in the online journal)

1. Introduction

Theoretical investigation and computational modeling of materials play an essential role in fields between the interface of condensed matter physics and materials science. Through the use and design of quantum-chemical methods, compounds such as transition-metal nitrides (TN_x) and carbonitrides (TCN_x) have been studied as superhard materials [1, 2] and most recently as 2D materials [3]. On another note, the discovery of graphene in 2004 [4] has been imperative for engineering 2D materials. Recently, the field has shifted its attention toward nanosheets such as silicene, phosphorene, germanene and stanene, [5] or functional 2D materials such as transition-metal dichalcogenides, (e.g. MoS_2, $MoSe_2$) [6].

The unique and exotic properties of transition-metal nitrides (TN_x) and carbonitrides (TCN_x) have drawn the attention of various communities within the interface of condensed matter physics, catalysis and materials science. Advances have been achieved by theoretically and experimentally exploring ReC_x and ReN_x compounds. Further investigation of ReN_x compounds [7–11] drove the field toward the synthesis of Re_2N [7], Re_3N, ReN_3 [9], the prediction of ReN_2 [8] and its

synthesis [9]. In parallel, ReC_x have been explored through the synthesis of Re_2C [12] and quantum-chemical calculations of ReC_2 [13]. However, nothing more is known about rhenium carbonitrides (ReC_xN_x).

In a recent report, two possible structures were calculated for ReCN through a density functional theory (DFT) first-principles approach. The authors predict ReCN to be a superhard material, comparable to other transition-metal carbonitrides [14]. Another *ab initio* study of ReCN shows it is possible to obtain it as a 2D-material [15]. Until now, further investigation of ReCN remains undone. Nonetheless, there is reason to suspect that rhenium carbonitride could pose potential applications in future electronic devices composed of different functional materials, such as Van der Waals heterostructures [14, 15]. Additionally, it would be interesting to evaluate this transition metal carbonitride as a topological insulator, as Re-based compounds have now been introduced in this class of materials [16, 17].

It will undoubtedly result useful to experimentalists and theorists alike to hold a firm understanding of the material and it is properties. Hence, a theoretical approach using an effective and versatile tight-binding method is desirable, as it is possible to reduce the complexity of a system to a few physical and chemical parameters. The tight-binding model can provide significant physical and chemical insight with respect to the electronic properties of molecules and compounds.

Here, we aim to employ an economic, simple and effective semi-empirical model to obtain insight into the electronic properties of ReCN. The physics of this material is discussed within the extended Hückel tight-binding (EHTB) framework [18, 19]. This quantum-chemical method has been known to successfully predict electronic properties of molecules and extended solids, such as filled skutterudites [20, 21], semi and superconductors, [22–24] and most recently, 2D materials such as group-IV nanosheets, offering a remarkably reliable and computationally economic description when compared to DFT [25]. Additionally, based on EHTB and its relationship to MO theory, we will carry out a Mulliken population analysis and evaluation of crystal field splitting (CFS). The value of such analysis resides in the opportunity of unraveling interesting properties in terms charge density and distribution while providing insight into the bonding properties of ReCN. We present the first report to look into the chemical bonding properties of ReCN and discuss the physics of the system in a language accessible to the broader community.

The EHTB method provides a feasible tool to approximate physical properties of materials, with a systematic and transparent execution of the calculations. It is reasonably simple to build upon tight-binding models of solid-state systems, justifying the motivation to model ReCN with methods alternative to DFT.

This article is organized as follows. First, we discuss the construction of our model based on the EHTB framework in section 2. The rhenium carbonitride structure and details of our numerical calculations are introduced in section 3, which includes the EHTB parameters used in our study. We continue to discuss our results in section 4, including band structure, DOS and CFS. Finally, our work is summarized and conclusions are drawn in section 5.

2. Extended Hückel tight-binding

A brief description of the EHTB formalism is provided. This method is a semi-empirical approach to solving the many body Schrödinger equation based on the variational theorem and the LCAO method, i.e.

$$\Psi_\alpha = \sum c_\alpha \phi_j, \tag{1}$$

where $\Psi_\alpha = \mathrm{MO}(\alpha)$ and $\phi_j = \mathrm{AO}(j)$. Additionally, C_{ij} are called the molecular orbital (MO) coefficients. They may be either positive or negative and their magnitude is closely related to the weight of the atomic orbital (AO) in that MO. In our EHTB calculations we consider the valence AO of each atom in our solid.

These AO are assumed to be real functions and are normalized such that the probability of finding an electron in ϕ_i is one, $\langle\phi_i|\phi_i\rangle = 1$. The MO are orthonormal, such that $\langle\Psi_\alpha|\Psi_\beta\rangle = \delta_{\alpha\beta}$ in bracket notation.

In the eigenvalue equation, ϵ_α is the energy that measures the effective potential exerted on an electron located in the αth Ψ_α. $\hat{H}\Psi_\alpha = \epsilon_\alpha\Psi_\alpha$. The coefficients are chosen such that the energy is minimized

$$\epsilon_\alpha = \langle\Psi_\alpha|\hat{H}|\Psi_\beta\rangle. \tag{2}$$

The obtained system of linear of Hückel equations is given by

$$\sum_{i,j} (H_{ij} - \epsilon_\alpha S_{ij})\ C_{ij} = 0 \tag{3}$$

with $i, j = 1, 2, 3$ ...

In order to solve the set of Hückel equations, we introduce some assumptions according to the EHTB method.

The diagonal elements of $\hat{H}$ are taken to be equal to the ionization energy of an electron in the ith valence ϕ of the isolated atom in the appropriate state, i.e. valence state ionization potential (VSIP), expressed as $H_{ii} = -\mathrm{VSIP}(\phi_j) = \epsilon_{\mathrm{onsite}}$.

The off-diagonal elements of $\hat{H}$ are evaluated according to a modified Wolfsberg–Helmholtz relation [26], given by

$$H_{ij} = \mathcal{K}\ S_{ij}\left(\frac{H_{ii} + H_{jj}}{2}\right), \tag{4}$$

where S_{ij} is the matrix of overlap integrals, $S_{ij} = \langle\phi_i|\phi_j\rangle$. In this work, $\mathcal{K} = 1.75$.

For our basis set, the valence atomic valence orbitals are approximated with Slater-type orbitals (STOs), of a single type for s and p and double zeta for d orbitals:

$$\phi_{s,p} = r^{n-l}\mathrm{e}^{(-\varsigma r)}Y(\theta, \omega), \tag{5}$$

$$\phi_d = r^{n-l}(C_1\mathrm{e}^{(-\varsigma r)} + C_2\mathrm{e}^{(-\varsigma 2r)})Y(\theta, \omega), \tag{6}$$

where $n =$ the principal quantum number, $r =$ the distance of the electron from the nucleus, ς the orbital exponent and $Y(\theta, \omega)$ is the angular part of the wave-function (real harmonics). It should be noted that ς may be obtained by applying the

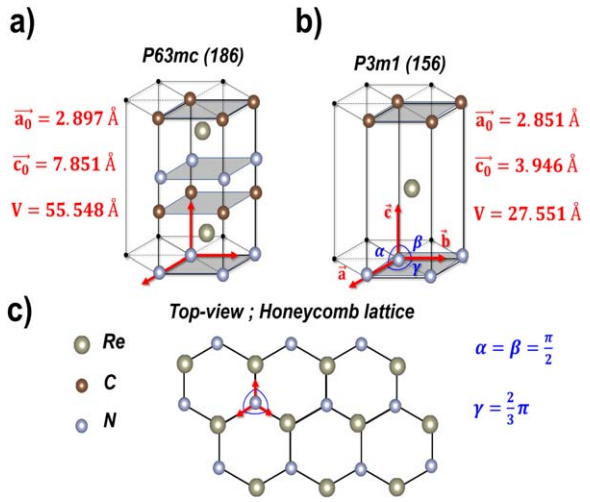

Figure 1. Unit cells in real space are shown for (a) the P6m3 structure, with given primitive vectors and cell volume as shown and equivalent values for (b) the P3m1 structure. An extended top-view is shown in (c) in order to illustrate the honeycomb lattice ReCN forms, although the physics of such system is not discussed in our work.

variational theorem to the equation above, however for the purpose of our study ς_1, ς_2, C_1, C_2 are taken as constants.

3. Calculation details

Rhenium carbonitride is a ternary compound that crystallizes in the P63mc (186) and P3m1 (156) space groups. The Bravais lattice is hexagonal for both structures, with the following Wyckoff positions: (a) P63mc; Re in 2 b (1/3, 2/3, 3/4), C in 2 a (0, 0, 2/25), N in 2a (0, 0, 1/2); (b) Re in 1 b with (1/3, 2/3, 1/2), C in 1 a with (0, 0, 1/2) and N in 1 a with (0, 0, 9/10). The primitive vectors are given by $\mathbf{a} = 2.857$ Å and $\mathbf{c} = 7.785\,1$ Å for P36mc (186); $\mathbf{a} = 2.851$ Å and $\mathbf{c} = 3.914$ Å for P3m1 (156). The unit cell volumes for the were 55.498 Å^3 and 27.551 Å^3 respectively. The structures used in our calculations were modeled using the Avogadro open-source package and optimized though Avogadro's built-in universal force field optimization tool [27]. We note that P3m1 is the unit cell that is reported to be extended to form a supercell, forming 2D-ReCN. For clarity, we describe that the view 'from above' of ReCN would form a honey-comb lattice, similar to transition-metal compounds such as MoS_2 [6]. However, discussing the monolayer is beyond the scope of this work. A schematic of the unit cells in real space is shown in figure 1.

Basis sets of 6*s*, 5*d* STOs were used for Re atoms and 2*p* STO were used for C and N atoms in our calculations. The atomic parameters used in our EHTB calculations were obtained from S. Alvarez who previously extracted them from *ab initio* calculations [28]. These parameters are shown in table 1. We used 100 *k* points for our calculations, sampling the first Brillouin zone (FBZ) as shown in figure 2. The values for energy ϵ (eV) versus *k* were plotted ranging from Γ (0, 0, 0) to M (1/2, 0, 0) to K (1/3, 1/3, 0) to Γ (0, 0, 0) to Z (0, 0, 1/2) to L (1/2, 0, 1/2) to H (1/3, 1/3, 1/2) Z (0, 0, 1/2). Electronic structure calculations were done using code written by Landrum and Glassy [29, 30].

Table 1. Atomic parameters used in EHTB calculations. The *d* orbitals for Re are given as a linear combination of two Slater-type orbitals. Each exponent ς_{ij} is followed by a weighting coefficient [31].

Atom	Orbital	H_{ii}	ς_{i1}	C_1	ς_{i2}	C_2
Re	6s	−9.3600	2.3980			
	6p	−5.9600	2.3720			
	5d	−12.7600	0.6382	5.3430	0.5653	2.2770
C	2s	−21.4000	1.6250			
	2p	−11.4000	1.6250			
N	2s	−26.0000	1.9500			
	2p	−13.4000	1.9500			

4. Results and discussion

4.1. Bond length

By means of the EHTB method, band structure calculations were carried out for ReCN in the P63mc and P3m1 phases. First, it is important to stress that our calculations yield bond lengths comparable to DFT studies by Fan [14] and Guerrero using the using a generalized gradient approximation method [15]. The bond lengths are seen in table 2.

The above table shows the comparison between bond lengths of the three studies. To further validate our model, we compare the distance between the C and N planes in the ReCN unit cell. In our model, the atomic distance between the C and N plane is 2.517 Å, while Guerrero [15] reports a distance of 2.509 Å. This distance is significant in the ReCN compound, as it indicates that there is no bond between the C and N atoms within the same unit cell, in a sense analogous to the two S atoms in MoS_2 [6].

4.2. Band structure

With regards to band structure, the Fermi level (ϵ_f) was calculated for 100 *k* points sampling the FBZ based on an ordering of 629 crystal orbitals occupied by 16 electrons in the unit cell. The calculated electronic band structures $\epsilon(k)$ are shown in figure 3, where the Fermi level is indicated by a blue line in the band structure diagrams. It is important to highlight that an indirect band gap of $\epsilon_g = 0.62$ eV is obtained for ReCN-P63mc at $M - K$, while a direct band gap $\epsilon_g = 0.49$ eV is obtained for the ReCN-P3m1 structure, situated at *H*. These results are in good quantitative agreement with previous studies, reporting band gaps of 0.67 eV for ReCN-P63mc and 0.73 eV [14], 0.51 eV [15] for ReCN-P3m1. Although EHTB is a semi-empirical method, there is a strong consensus of the band gap values between the two approaches. However it is worth-while to note that computational methods have their flaws. While DFT calculations may underestimate band gap values, EHTB calculations may overestimate them. The reasonable agreement between the band gap values obtained by the different approaches indicate that similar values are to be expected from experimental measurement. Hence, this consensus should suffice the understanding of the electronic properties of the yet to be

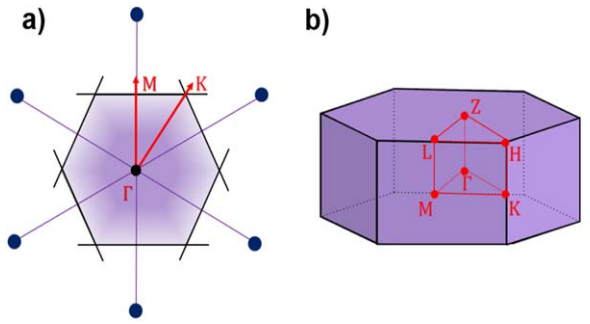

Figure 2. First Brillouin zone in reciprocal space is shown for ReCN as (a) projection and (b) complete FBZ.

Table 2. Bond length comparison between EHTB calculations and literature.

Structure	Re-C Å	Re-N Å	C–N Å
EHT	2.107	2.081	1.408
DFT 1[14]	2.109	2.082	1.401
DFT 2[15]	2.103	2.077	1.413

synthesized semiconductor. Spin–orbit coupling was not taken into account in these band structure calculations, and it is worth mentioning that it could have an effect on the bands, particularly unfolding them and broadening the ϵ_g. It is necessary to analyze those orbitals that are close to the ϵ_f since they form a hybridized band between Re *d* orbitals and C *p* and N *p* orbitals.

4.3. Density of states (DOSs)

DOSs is defined as the number of crystal levels between an energy range $\epsilon + d\epsilon$. This provides real-space insight into the orbital occupation levels over the FBZ in the compound and unravels chemical properties of ReCN.Total density of states plots are shown in figure 4. The DOS curves shown in figure 4 are derived from the band structure, as DOS(ϵ) is proportional to the inverse of the slope of the $\epsilon(k)$ curves in the band structure plots. For clarity, we can see that the integral of DOS up to ϵ_f is the number of occupied MOs. Notice then that the absence of a DOS peak in both (a) and (b) near the Fermi level ϵ_f is a clear indicator of semiconductor behavior, as it represents that electrons are prohibited from occupying these energy states. The semiconducting behavior in a material is strongly related to the valence electron count, which is 16 for ReCN. From the DOS curves it can be seen that the contributions at the Fermi level are due to 5*d* orbitals in Re, 2*p* in N and 2*p* in C. Doping of ReCN by substituting atoms could also pose changes in electron bands, by increasing or reducing its conductivity.

Fractional PDOS plots are provided in figure 5 for a more detailed understanding of DOS contributions from Re, N and C for the (a) P63mc and (b) P3m1 phases.

Average charge density shows preference toward N due to its electronegativity, secondly to Re and minimally to C. It is important to stress that in transition metal compounds and complexes such as ReCN, partially filled *d* orbitals are responsible for a range of physical properties. Thus, it would result interesting to investigate the influence of the 5*d* orbitals in the Re atom to the electronic-structure dependent properties, such as thermoelectric and magnetic properties.

Comparing to literature [14, 15], one can readily see that there is reasonable agreement between our calculations and the ones obtained by the DFT approach. Fan [14] briefly compares the DOS of ReCN to ReN_2 and ReC_2 , which are high density of state materials. This portrays ReCN as an interesting candidate for technological applications as it is a semiconductor, whereas the other compounds discussed are likely to be superconductors. Guerrero also sees semiconductor behavior for the ReCN bulk structure [15]. Stoichiometry should play a strong role in the DOS as in the bonding properties of the compound. In section 4.1 we discussed the bond lengths and the distance between the C and N planes, in agreement with DFT reports. As mentioned, there is no direct C and N interaction in the unit cell, due to steric effects, i.e. the impossibility of C and N to reach bonding distance, possibly due to the stronger bonding between the Re and N atoms, as is to be expected since N is more electronegative. It is clear that this null interaction between C and N contributes to the stability of the compound, maximizing bonding and ultimately lowering the DOS. The fact that C and N do not interact may be the key as to why ReCN is a semiconductor versus its successors ReC_2 and ReN_2, which have notable metallic properties.

4.4. Crystal field orbital splitting

In order to better understand the chemical nature and bonding properties of ReCN in terms of localized atomic charge, Mulliken population analysis was performed. Beside gaining insight into the molecular bonding and antibonding properties of ReCN, we relate Mulliken population analysis to the CFS (within the general ligand field theory) of *d* orbitals in Re atoms, a concept well-known from Group Theory. This was achieved by calculating the net charge migration based on an ordering of 629 crystal orbitals occupied by 16 electrons in the unit cell for P63mc and 2915 crystal orbitals with 34 electrons in the unit cell for P3m1. Our calculations yield a total charge migration of 1.866 344 e in the P63mc structure and 1.241 86 e in the P3m1 structure. The average net charges for the Re, C and N atoms are as follows: 0.977 877, 0.284 175, −1.262 052 for P63mc and −0.029 523, 0.048 506, −0.018 983 for P3m1. It can be seen that this charge migration can be attributed to the anionic behavior in N atom. It is also imperative to understand that ReCN is a possible compound due to the cationic nature of Re and anionic nature of C and N. Moreover, the bond formation is given by N → Re σ and π donation, C → Re σ and π donation, Re–Re bonds are formed by the overlap of $d_{x^2-y^2}$ and d_{xy} orbitals, forming a δ bond, maximizing bonding and reaching stability. Reiterating, bonding is maximized forming a strong Re–N bond, and no bond between C and N.

Due to the ionic nature of ReCN, it is worthwhile focus on the d orbitals in the Re atom from the LFT standpoint (ligand field theory). As mentioned, ReCN crystallizes in

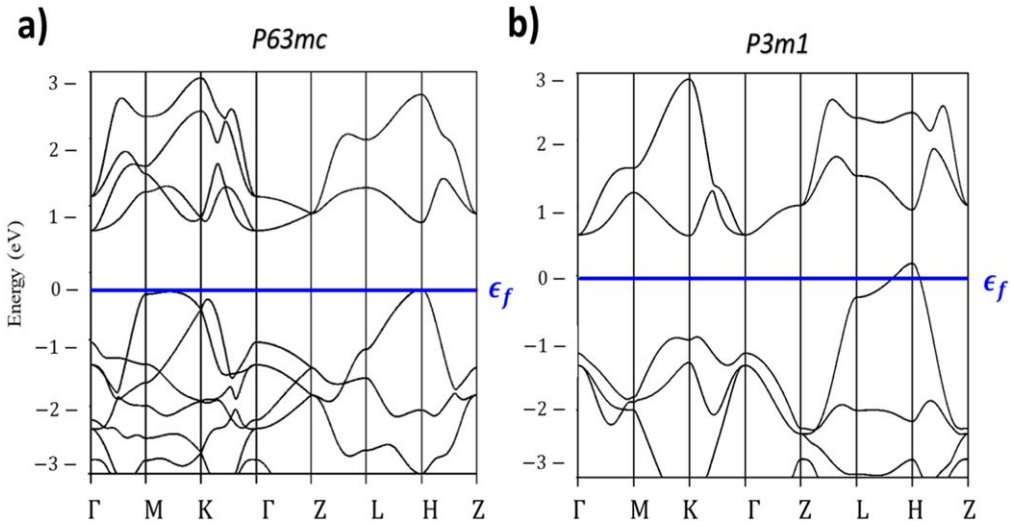

Figure 3. The electronic band structure is shown in (a) for ReCN P63mc and (b) ReCN P3m1. EHTB Calculations yield $\epsilon_f = 0.62$ and $\epsilon_f = 0.49$ eV respectively.

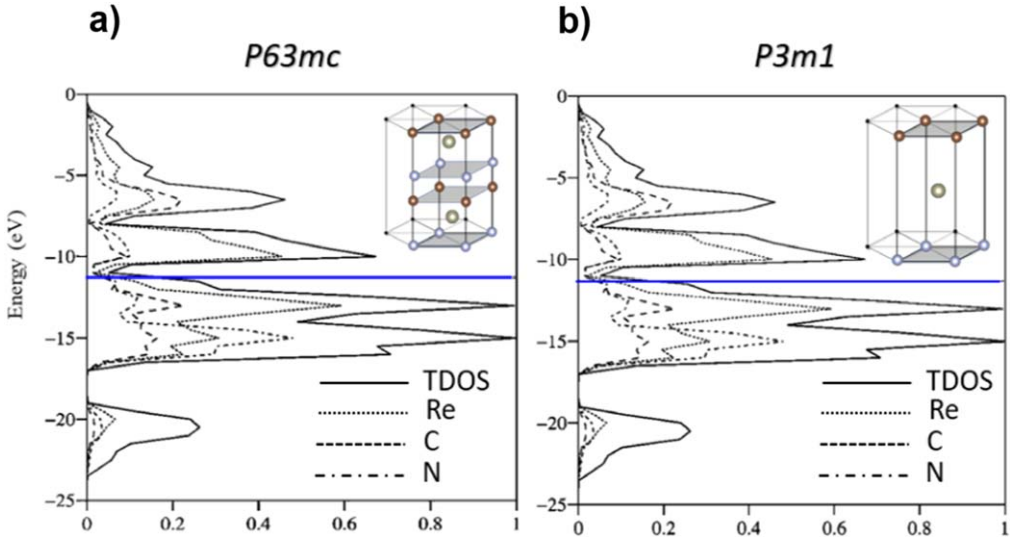

Figure 4. Total density of states is shown for (a) ReCN P63mc and (b) P3m1. The solid line is the TDOS (sum of all contributions) while the dotted lines depict the contributions of individual atoms. Fermi level is indicated by a blue line. PDOS is shown in figure 4.

space groups P63mc and P3m1 with a tetragonal primitive cell. Hence, the effect of tetragonal crystal field is to lift the five-fold degeneracy of *d* orbitals in Re atoms, providing distinct energy values in the crystal. Note that CFS occurs as consequence of a change in an electron's energy when the *d* orbital is located in a region of either high electron density, in which the energy increases, or lower in the contrary case. These values are ordered from lowest—highest energy: (a) P63mc: d_{xy}, d_{yz}, d_{xz}, $d_{x^2-y^2}$, d_z^2 and (b) P3m1: d_{xz}, d_{yz}, d_{xy}, d_z^2, $d_{x^2-y^2}$. The *d*-orbital splitting is shown in figure 6 in accordance to our analysis. For both structures, the five-fold degeneracies break into 3 t_{2g} below 2 e_g orbitals. This is to be expected for a Re atom submerged in a tetragonal configuration as in in agreement with Group Theory [32].

Clearly, the first orbital filled is the d_{yz} immediately followed by the d_{xy} orbital. These are evidently bonding orbitals, and the filling of orbitals obey Afbau's and Hund's rules. The presence of unpaired electrons (typically one in semiconductors) suggest a high spin behavior, leading to predict paramagnetic behavior in ReCN. Another indicator of high-spin properties is the fact that ReCN is tetragonal with no bonding between C and N in the unit cell.

Comparing (a) and (b) in figure 6, one notices a difference in the order of electron occupation of *d* orbitals between the two structures. Notice that although both structures depict the tetragonal CF configuration, (3 t_{2g} below 2 e_g), structure P63mc undergoes a loss of symmetry. The splitting of *d*-energy levels can lead to degenerate electron configurations (i.e. electron distributions) and atom arrangements [32, 33]. indicates that the structure might be Jahn–Teller active, meaning high-spin character is to be expected [32]. This would imply that ReCN holds paramagnetic properties. In order to reveal the full landscape of the magnetic properties of

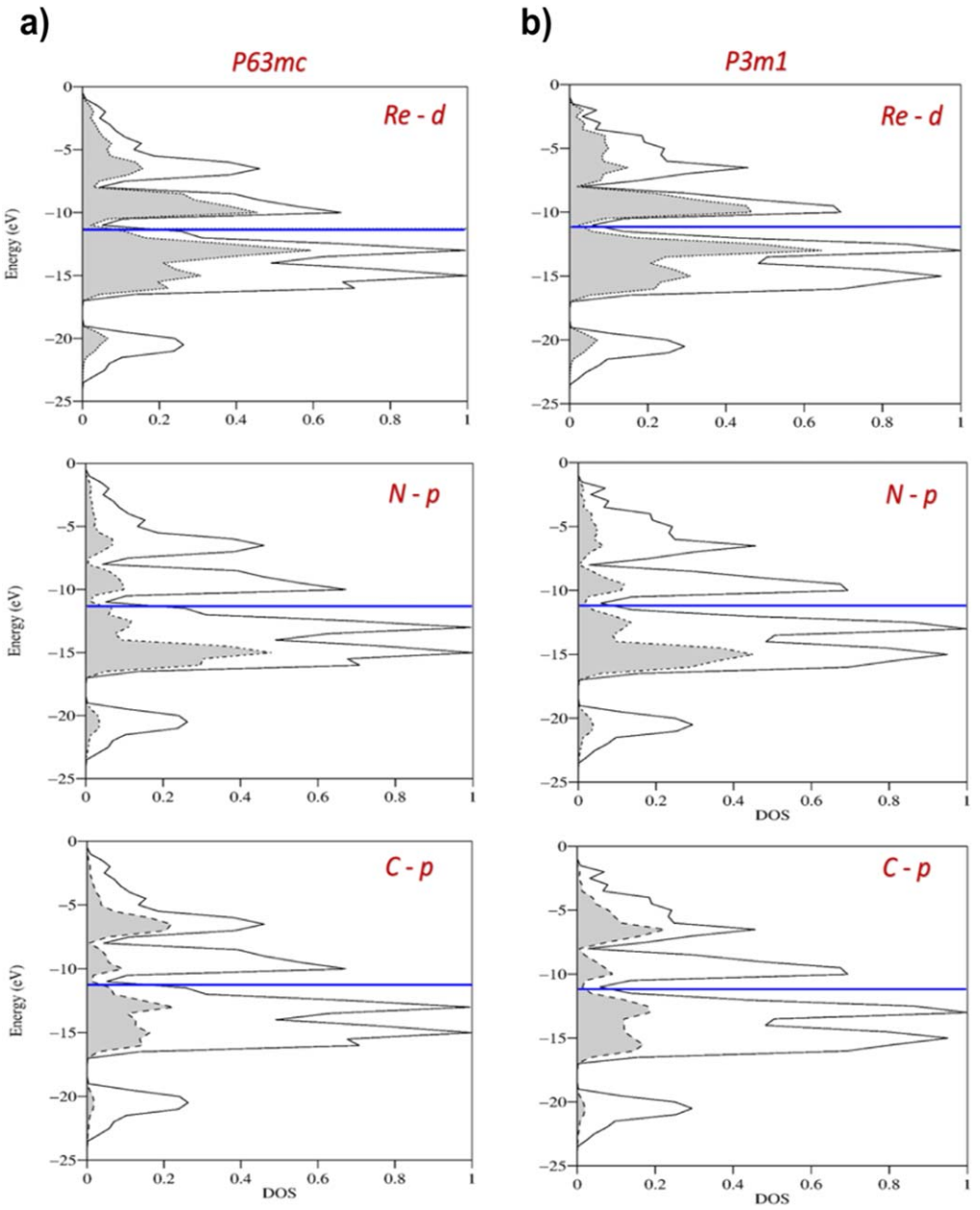

Figure 5. Projected density of states are shown to differentiate which atoms and orbitals contribute most to the Fermi level, indicated by a blue line. Semiconductor behavior is observed with a dominant contribution from d orbitals in Re atoms.

ReCN, incorporating a spin–orbit coupling term to the EHTB Hamiltonian is required. This is especially true when dealing with strongly-correlated atoms such as Re.

A different but equivalent way of saying this in solid-state jargon is to say it undergoes Peierls distortion [34]. To understand this, we start at the five-fold degeneracies. The degeneracies are defined simply as $\epsilon(k) = \epsilon(-k)$ for any k in the FBZ, near degeneracies correspond to k' right off of ϵ_f. For partially filled $\epsilon(k)$ bands, as the P63mc system tends to stability, a deformation takes place. The partial filling leads to an electron–phonon coupling, opening a gap at ϵ_f by stabilizing one orbital and destabilizing another. This deformation occurs in order to minimize the energy of the system, maximizing bonding and resulting in a loss of symmetry. This is in agreement with our band structure and DOS as ϵ_g is larger in P63mc (0.62 eV) than in P3m1 (0.49 eV). The Peierls distortion could potentially explain why the P63mc structure could not yield the ReCN monolayer—it would collapse [15]. The P3m1 structure does not present this Peierls distortion, conserving symmetry.

Peierls and Jahn–Teller distortion in transition metal compounds has drawn recent attention. Recently, it has been predicted that Peirels distortion is responsible for the transitions between phases in ReS_2 [35]. A more detailed study of Peierls and Jahn–Teller transitions in ReCN would result valuable, as they could unravel information regarding the magnetic nature of the transition metal compound.

It is imperative to stress that although presented in a semi-qualitative manner, the implications that CFS has on the physical properties are significant. However, we wish to

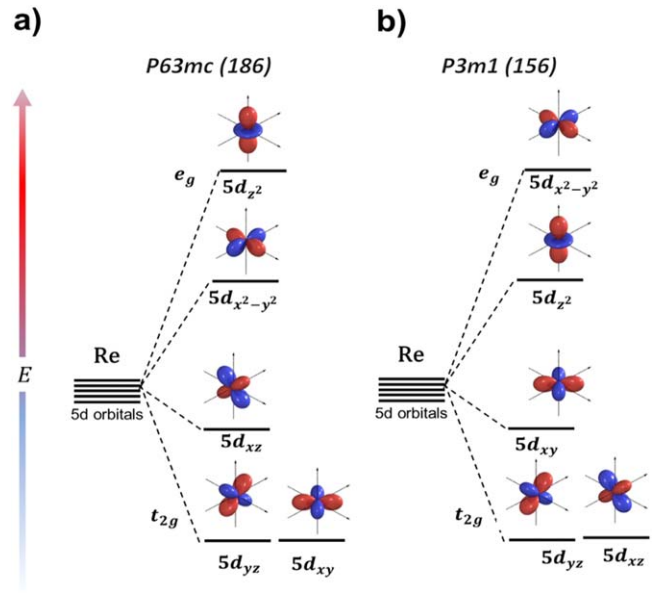

Figure 6. Schematic illustration of crystal field splitting (CFS) of d orbitals in Re atoms into (a) e_g, t_{2g} symmetry groups in P53mc structure and (b) e_g and t_{2g} symmetry groups P3m1 structure.

highlight that spin–orbit coupling was not taken into account in this study, and it is necessary to obtain a complete understanding of spin-related phenomena such as magnetism when many electrons are involved (e.g. 75 in Re). Therefore, we hope our study will serve as a primer for further investigation involving spin–orbit coupling.

5. Summary and conclusions

In this work, we studied the electronic structure of rhenium carbonitride (ReCN) by means of the EHTB method. The construction of a feasible EHTB-Hamiltonian was described and the semiconductor properties were discussed for ReCN P63mc and ReCN P3m1. From the band structure it can be seen that P63mc and P3m1 hold indirect ($M-K$) and direct (H) band gaps of 0.62 and 0.49 eV respectively. The obtained results were compared with those obtained though finer and computationally more expensive calculations in order to validate the EHTB approach. The null interaction between the C and N atoms in the unit cell are what aid the maximization of bonding, lowering the DOS and give ReCN semiconductor properties instead of a metallic nature. Additionally, CFS of the *d* orbitals was analyzed for the Re atom of each structure. Tetragonal crystal field splitting is observed in both structures, with five-fold degeneracies breaking into groups 3 t_{2g} below 2 e_g. The P63mc structure shows a loss of symmetry caused by Peierls distortion to minimize the energy of the system, broadening the gap at the Fermi level. We hope our study will motivate further theoretical characterization of the yet-to-be synthesized ReCN, with an invitation to make use of semi-empirical methods such as EHTB and others alike.

Acknowledgments

The authors acknowledge DGTIC-UNAM for computational support. EP acknowledges partial support from DGAPA-PAPIME 110717 as part of the JI2017 program. AR is supported by DGAPA-PAPIIT IN112917 and LANCAD-UNAM-DGTIC-084. Additionally, EP thanks O A Ramírez-Ramírez and A Noguerón-Aramburu for insighful discussions. DG acknowledges support from LANCAD-UNAM-DGTIC-041.

ORCID iDs

Etienne I Palos https://orcid.org/0000-0003-1352-8886
Armando Reyes-Serrato https://orcid.org/0000-0001-6741-8813

References

[1] Veprek S 1999 The search for novel, superhard materials *J. Vac. Sci. Technol.* A **17** 2401
[2] Jhi S H, Ihm J, Louie S G and Cohen M L 1999 Electronic mechanism of hardness enhancement in transition-metal carbonitrides *Nature* **399** 132
[3] Zhou B, Dong S, Wang Z, Zhang K and Mi W 2017 An sd^2 hybridized transition-metal monolayer with a hexagonal lattice: reconstruction between the Dirac and kagome bands *Phys. Chem. Chem. Phys.* **19** 8046
[4] Novoselov K S, Geim A K, Morozon S V, Jiang D, Zhang Y, Dubonos S V, Grigorieva I V and Firsov A A 2004 Electric field effect in atomically thin carbon films *Science* **306** 666–9
[5] Bhimanapati G R *et al* 2015 Recent advances in two-dimensional materials beyond graphene *ACS Nano* **9** 11509–39
[6] Manzeli S, Ovchinnikov D, Pasquier D, Yazyev O V and Kis A 2017 2D transition metal dichalcogenides *Nat. Rev.: Mater.* **2** 17033
[7] Li Y and Zheng Z 2009 New potential super-incompressible phase of ReN_2 *Chem. Phys. Lett.* **474** 93
[8] Friedrich A, Winkler B, Bayarjargal L, Morgenroth W, Juarez-Arellano E A, Milman V, Refson K, Kunz M and Chen K 2010 Novel rhenium nitrides *Phys. Rev. Lett.* **105** 085504
[9] Soto G, Tiznado H, de la Cruz W and Reyes A 2014 Synthesis of ReN_3 thin films by magnetron sputtering *J. Mater.* **2014** 745736
[10] Kawamura F, Yusa H and Taniguchi T 2012 Synthesis of rhenium nitride crystals with MoS_2 structure *Appl. Phys. Lett.* **100** 251910
[11] Soto G 2012 Computational study of Hf, Ta, W, Re, Ir, Os and Pt pernitrides *Comput. Mater. Sci.* **61** 1
[12] Zhao Z *et al* 2010 Bulk Re_2C: crystal structure, hardness, and ultra-incompressibility *Cryst. Growth Des.* **10** 5024
[13] Zhang M, Yan H, Zhang G, Wei Q and Wang H 2012 First-principles calculations on crystal structure and physical properties of rhenium dicarbide *Solid State Commun.* **152** 1030
[14] Fan X, Li M M, Singh D J, Jiang Q and Zheng W T 2015 Identification of a potential superhard compound ReCN *J. Alloys Compd.* **631** 321

[15] Guerrero-Sánchez J, Noboru Takeuchi and Reyes-Serrato A 2017 *Ab-initio* study of ReCN in the bulk and as a new two dimensional material *Sci. Rep.* **7** 2799
[16] Geim A K and Grigorieva I V 2013 van der Waals heterostructures *Nature* **499** 419–35
[17] Novoselov K S, Mishchenko A, Carvalho A and Castro Neto A H 2016 2D materials and van der Waals heterostructures *Science* **29** aac9439
[18] Hoffmann R 1963 An extended Hückel theory: I. Hydrocarbons *J. Chem. Phys.* **39** 1397
[19] Hoffman R 1964 An extended Hückel theory: II. Orbitals in the Azines *J. Chem. Phys.* **40** 274
[20] Galvan D H, Dilley N R and Maple M B 2003 Extended Hückel tight-binding calculations of the electronic structure of $YbFe_4Sb_{12}$, UFe_4 P_{12}, and $ThFe_4$ P_{12} *Phys. Rev.* B **68** 115110
[21] Galvan D H and Samaniego C 2004 Electronic structure calculations for $PrOs_4Sb_{12}$ filled skutterudite. A theoretical approach using extended Hückel tight-binding method *Phys. Rev.* B **70** 145108
[22] Matos M 1999 Electronic band structure of 3C–SiC from extended Hückel theory *J. Mol. Struct.: Theochem* **464** 129
[23] Matos M, Terra J and Ellis D E 2009 Semiempirieal electronic structure calculation on Ga and Pb apatites *Int. J. Quantum Chem.* **109** 849–60
[24] Galvan D H 1998 Extended Hückel calculations on cubic boron nitride and diamond *J. Mater. Sci. Lett.* **17** 805
[25] de Souza Martines A and Veríssimo-Alves M 2014 Group-IV nanosheets with vacancies: a tight-binding extended Hückel study *J. Phys.: Condens. Matter* **26** 1–7
[26] Wolfsberg M W and Helmholtz L 1952 The spectra and electronic structure of the tetrahedral ions MnO_4, CrO_4, and ClO_4 *J. Chem. Phys.* **20** 837
[27] Hanwell M D, Curtis D E, Lonie D C, Vandermeersch T, Zurek E and Hutchison G R 2012 Avogadro: an advanced semantic chemical editor, visualization, and analysis platform *J. Cheminformatics* **4** 17
[28] Alvarez S 2000 Tables of parameters for extended Hückel calculations Universitat de Barcelona. Updated 2012
[29] Landrum G A and Glassey W V Bind (ver 3.0). bind is distributed as part of the YAeHMOP extended Hückel molecular orbital package and is freely available
[30] Landrum G A Viewkel (ver 3.0). Viewkel is distributed as part of the YAeHMOP extended Hückel molecular orbital package and is freely available
[31] Alvarez S 1993 Table of parameters for extended Hückel calculations, Universitat de Barcelona
[32] Cotton F A 1990 The crystal field theory *Chemical Applications of Group Theory* 3rd edn (New York: Wiley) pp 282–7
[33] Jahn H A and Teller E 1937 *Proc. R. Soc.* A **161** 220–35
[34] Hoffmann R 1988 *Solids and Surfaces: A Chemist's View of Bonding in Extended Structures* (New York: VCH) pp 92–106
[35] Choi J-H and Jhi S-H 2018 *J. Phys.: Condens. Matter* **30** 105403